

# Aerial Tool Operation System using Quadrotors as Rotating Thrust Generators

Hai-Nguyen Nguyen, Sangyul Park and Dongjun Lee

**Abstract**—We propose a new aerial tool operation system consisting of multiple quadrotors connected to a tool by spherical joints to perform tool operation tasks. We model the system and show that the attitude dynamics of each quadrotor is decoupled from the tool dynamics, so that we can consider the quadrotors as thrusters and control the tool by adjusting the orientation and magnitude of these thrusters. We also show that the 6-DOF tool dynamics could be under-actuated or fully-actuated, depending on the number of quadrotors attached to the tool and the geometric configuration of their attachments. We then design control laws for the tool-tip position/orientation tracking of the (under-actuated) tool system with two quadrotors and the (fully-actuated) tool system with three quadrotors. We use Lyapunov approach to find the desired thrust command for each quadrotor while also taking into account the spherical joint limits in a form of constrained optimization. Simulation and implementation results are performed to support the theory.

## I. INTRODUCTION

Recently, quadrotors have attracted tremendous attention from research community and general public alike, due to their agile performance and affordability. Many strong results have been achieved for the motion control of the center of mass position of the quadrotors, which is the backbone of many powerful applications such as aerial photography, remote movie shooting, landscape survey or surveillance. See [1] for a recent development.

With the plethora of control results for the quadrotor motion control, it can now be expected that the research focus will be broadened to applications requiring interaction of quadrotors with their surrounding environment, external objects or even between quadrotors themselves. However, there are relatively rare results for this purpose, e.g., hybrid position/force control [2] and tool operation [3], [4], [5] using a single quadrotor, cable-suspended payload transport [6], [7], contact task using attached ducted-fan UAVs [8], [9], and quadrotor-manipulator systems [10].

Among these, we believe the idea of achieving aerial tool operation by using a tool rigidly-attached to a quadrotor with the quadrotor acting as the direct actuator [3], [4], [5] is promising, since with a simple un-actuated tool (e.g., screw-driver), the system would be more affordable and also can accommodate higher interaction force (or payload) with longer flight-time (as compared to, e.g., quadrotor-manipulator systems with heavy multi-DOF arm). However, we also found in [3], [4], [5] that possible tasks achievable by using this simple rigid-tool attached to the quadrotor would be limited, since the tool operation requires simultaneous control of the 6-DOF quadrotor position and orientation,

The authors are with the Department of Mechanical & Aerospace Engineering and IAMD, Seoul National University, Seoul, Republic of Korea, 151-744. Email: {hainguyen,sangyul,djlee}@snu.ac.kr

Corresponding author: Dongjun Lee

Research supported in part by the Basic Science Research Program (2012-R1A2A2A0-1015797), the Global Frontier R&D Program on Human-Centered Interaction for Coexistence (NRF-2013M3A6A3079227), and the Brain Korea 21 Plus Project in 2014 (F14SN02D1310) of the National Research Foundation (NRF) by the Korea Government (MEST)

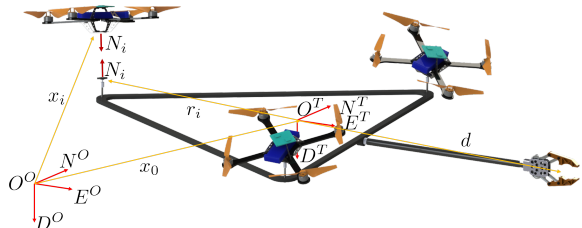


Fig. 1. Spherically-connected multiple-Quadrotor Tool (SmQT) system:  $\{O\} := \{O^O, E^O, D^O\}$  and  $\{T\} := \{N^T, E^T, D^T\}$  are the fixed and tool frames with  $D^O$ -axis being the gravity direction.

yet, the quadrotor itself is under-actuated with only four actuators. This issue of under-actuation, in fact, turns out to be able to create unstable internal dynamics (with the tool attached below the quadrotor) or even trigger finite-time escape, thereby, limiting its practical applicability. Refer to [3], [4] for more details.

To overcome this limitation of the single-quadrotor tool operation system, in this paper, we propose a new aerial tool operation system consisting of multiple quadrotors connected to a tool by spherical joints. See Fig. 1. With the attitude dynamics of each quadrotor decoupled from the tool dynamics, we can then control the tool by adjusting the attitude of the quadrotors and the magnitude of their thrusts. In other words, we can utilize multiple quadrotors as distributed rotating thrust generators for the tool. This proposed aerial tool system is promising to overcome some key problems of current aerial manipulation systems, that are, 1) can *extend limited interaction force* (or payload), short flight-time by utilizing multiple quadrotors and a simple un-actuated tool; and 2) can *resolve the under-actuation issue* of a single quadrotor system by selecting suitably the geometric configuration of multiple distributed thrusters/quadrotors.

Another benefit of this proposed system, not yet clear at first glance, is that the tool system is more *robust under side-way gust* since the tool dynamics would not be disturbed as the quadrotors tilt to counteract the wind gust. For typical quadrotor-manipulator (QM) systems, however, the disturbance on the quadrotor attitude will consequently impact on the attitude of the manipulator and therefore the performance of the QM system. How to improve robustness of QM systems under wind gust is rather challenging since 1) for a simple QM system, e.g., system with 2-DOF arm, the disturbance from quadrotor attitude may not be completely compensated by the arm movement; 2) for a complex QM system with a dexterous multi-DOF arm, the compensation motion of the arm may in turn induce further disturbance on the quadrotor platform. This, in fact, defines a clear advantage of this spherically-connected quadrotor tool system against other rigidly-connected QM systems.

The main contribution of this paper is the dynamics analysis and the basic pose tracking control design of this Spherically-connected multiple-Quadrotor Tool (SmQT)

system. More specifically, we first provide the dynamics modeling of the total system and characterize the condition for the 6-DOF tool to be fully-actuated while respecting the motion limits of the spherical joints. This condition in fact turns out to depend on the mechanical design of the system (i.e., number of quadrotors attached to the tool, geometric configuration of their attaching points and axes of their spherical joints). We then consider Spherically-connected 2-Quadrotor Tool (S2QT) system, which, although under-actuated along one direction (i.e., only 5-DOF of the 6-DOF tool is actuated), can still be made to track a desired tool-tip position trajectory with certain orientation; and also the Spherically-connected 3-Quadrotor Tool (S3QT) system, which, under the aforementioned mechanical design condition, becomes fully-actuated so that we can achieve full 6-DOF dexterous motion. For all these applications, we utilize Lyapunov approach to design the desired control wrench of the tool, and allocate that computed wrench to each quadrotor while respecting the spherical joint limits by solving a certain constrained optimization, whose structure turns out to be similar to the well-known problem of robot grasping with friction-cone constraint [11].

Some results relevant to our system are as follows. In [12], the authors use multiple quadrotors fixed to an object to extend payload limitation of the system, yet, the dynamics of the payload is still under-actuated as the thrust directions of the quadrotors are all aligned with each other. In [9], the authors propose a system of multiple ducted-fan UAVs rigidly-connected with each others to achieve full-actuation. The system of [9] yet is different from ours with their results not applicable to ours. In [6], [7], a cable-suspended system using multiple UAVs is considered, where the equilibrium pose of the suspended payload can be achieved by equilibrating the gravity wrench with the wrenches exerted by the cables from multiple UAVs. In these works, they assume that 1) the system is quasi-static, i.e., the inertial forces associated with the motions of the payload and the quadrotors are negligible, and 2) the cable attachment points, therefore UAVs, can be controlled kinematically regardless of the interaction between the payload and the UAVs. This in fact is in a stark contrast to our result here, where the full dynamics of the system including the dynamics interaction between the quadrotors and the tool need to be explicitly modeled and analyzed.

The rest of this paper is organized as follows. The dynamic model of the system is derived in Sec. II. The relation between full-actuation and mechanical design is analyzed in Sec. III. Two control design examples, tool-tip position/orientation tracking control of the S2QT system and S3QT system, are presented in Sec. IV along with relevant simulation and experimental results. Some concluding remarks are given in Sec. V.

## II. SYSTEM MODELING

### A. System Description

Consider a system consisting of  $n (\geq 2)$  quadrotors connected to a tool using spherical joints as shown in Fig 1. These spherical joints have limited range of motion, which can be represented as a reaching cone  $(p_i, \phi_i)$  with the center-axis unit vector  $p_i \in \mathbb{R}^3$  and the range of angle motion  $\phi_i \in \mathbb{R}$  ( $0 \leq \phi_i \leq \pi/2$ ) as shown in Fig 2. Then, we can define the spherical joint limit constraints as:

$$p_i^T \Gamma_i \geq |\Gamma_i| \cos \phi_i, i = 1, 2, \dots, n \quad (1)$$

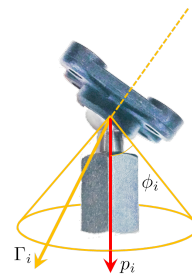


Fig. 2. Joint limit of spherical joint:  $p_i$  is the center-axis unit vector,  $\phi_i$  the allowable motion range, and  $\Gamma_i$  the quadrotor thrust in tool frame.

where  $\Gamma_i := \lambda_i R_0^T R_i e_3 \in \mathbb{R}^3$  is the quadrotor thrust in tool frame,  $R_0, R_i \in SO(3)$  are the attitudes of the tool and the  $i^{th}$  quadrotor with respect to the fixed frame,  $|\lambda_i| = |\Gamma_i| \in \mathbb{R}$  is the magnitude of the quadrotor thrust, and  $e_3 = [0; 0; 1]$  is the standard unit vector along the  $D$ -axis.

These constraints can be defined according to the mechanical limit of the spherical joints themselves or to avoid collision between the quadrotors and the tool. Note also that these constraints themselves require the body-frame thrusts generated by the quadrotors to be positive ( $\lambda_i > 0$ ).

In this work, we assume that each joint is attached at the center-of-mass of each quadrotor, which can be satisfied with the mechanical design shown in Sec IV-A. We then have the following relation between the center-of-mass position  $x_i \in \mathbb{R}^3 (i \geq 1)$  of the  $i^{th}$  quadrotor and the position  $x_0 \in \mathbb{R}^3$  of the tool in the fixed frame  $\{O\}$  as:

$$x_i = x_0 + R_0 r_i \quad (2)$$

where  $r_i \in \mathbb{R}^3$  is the attaching point of the  $i^{th}$  quadrotor represented in the tool frame  $\{T\}$ . See Fig. 1.

With (2) acting as constraints, the dynamics of each quadrotor and the tool can be written as:

$$\begin{aligned} m_i \ddot{x}_i &= -\lambda_i R_i e_3 + m_i g e_3 + N_i \\ J_i \dot{\omega}_i &= -S(\omega_i) J_i \omega_i + \tau_i \\ m_0 \ddot{x}_0 &= -\sum_{i=1}^n N_i + m_0 g e_3 + f_e \\ J_0 \dot{\omega}_0 &= -S(\omega_0) J_0 \omega_0 - \sum_{i=1}^n S(r_i) R_0^T N_i + \tau_e \end{aligned} \quad (3)$$

where  $m_i, J_i$  and  $m_0, J_0$  are the mass and inertia of the  $i^{th}$  quadrotor and the tool respectively,  $\omega_i, \omega_0 \in \mathfrak{so}(3)$  are their angular velocities,  $N_i \in \mathbb{R}^3$  is the constraint force between the  $i^{th}$  quadrotor and the tool,  $S(\omega)$  is a skew-symmetric matrix such that  $S(\omega)\nu = \omega \times \nu, \forall \omega, \nu \in \mathbb{R}^3$ , and  $f_e, \tau_e \in \mathbb{R}^3$  are the external force and torque acting at the center-of-mass of the tool represented in the fixed frame  $\{O\}$  and the tool frame  $\{T\}$ , respectively.

### B. Reduced Dynamics

By eliminating the constraint forces  $N_i$  in (3), we can reduce the dynamics (3) into the 6-DOF dynamics of the tool and the 3-DOF attitude dynamics of each quadrotor as follows. First, the 6-DOF tool dynamics is given by:

$$M \dot{\xi} + C + G = U + F_e \quad (4)$$

where  $\xi = [\dot{x}_0; \omega_0] \in \mathbb{R}^6$  is the 6-DOF translation/angular tool velocity,

$$M := \begin{bmatrix} \sum_{i=0}^n m_i I & -\sum_{i=1}^n m_i R_0 S(r_i) \\ \sum_{i=1}^n m_i S(r_i) R_0^T & J_0 - \sum_{i=1}^n m_i S^2(r_i) \end{bmatrix}$$

$$C := \begin{bmatrix} -\sum_{i=1}^n m_i R_0 S(\omega_0) S(r_i) \omega_0 \\ -\sum_{i=1}^n m_i S(r_i) S(\omega_0) S(r_i) \omega_0 + S(\omega_0) J_0 \omega_0 \end{bmatrix}$$

$$G := \begin{bmatrix} -\sum_{i=0}^n m_i g e_3 \\ -\sum_{i=1}^n m_i g S(r_i) R_0^T e_3 \end{bmatrix}, \quad F_e := \begin{bmatrix} f_e \\ \tau_e \end{bmatrix}$$

are the lumped inertia matrix, the Coriolis, the gravity and the external forcing terms of the tool dynamics, respectively,  $U := \bar{R}B\Gamma \in \mathbb{R}^6$  is the control action of the tool with  $\bar{R} := -\text{diag}[R_0, I] \in \mathbb{R}^{6 \times 6}$ ,

$$B(r) := \begin{bmatrix} I & I & \dots & I \\ S(r_1) & S(r_2) & \dots & S(r_n) \end{bmatrix}$$

$$\Gamma := \begin{bmatrix} \Gamma_1 \\ \Gamma_2 \\ \vdots \\ \Gamma_n \end{bmatrix} = \begin{bmatrix} \lambda_1 R_0^T R_1 e_3 \\ \lambda_2 R_0^T R_2 e_3 \\ \vdots \\ \lambda_n R_0^T R_n e_3 \end{bmatrix}$$

with  $r = (r_1, r_2, \dots, r_n)$  and  $I \in \mathbb{R}^{3 \times 3}$  being identity matrix. On the other hand, the attitude dynamics of each quadrotor is given by:

$$J_i \dot{\omega}_i = -S(\omega_i) J_i \omega_i + \tau_i \quad (5)$$

We can then see that the quadrotor attitude dynamics (5) is decoupled from the tool dynamics (4). Here, since the attitude dynamics of the quadrotors is typically faster than the tool dynamics, we can use the thrusts  $\Gamma_i = \lambda_i R_0^T R_i e_3 \in \mathbb{R}^3$  as the control input for the 6-DOF tool dynamics (4), that is, use the  $n$ -quadrotors as rotating thrust actuators for the 6-DOF tool dynamics (4).

We can also see that the structure of  $B(r) \in \mathbb{R}^{6 \times 3n}$  in (4) dictates whether we can generate an arbitrary control action  $U \in \mathbb{R}^6$  by using the thrust inputs  $\Gamma_i$  of the  $n$ -quadrotors. This structure of  $B(r)$  depends on the number of quadrotors and their attaching points  $r_i$  (see Fig. 1). In the next Sec. III, we show how the geometric design and the attachment of the spherical joints affect the control actuation for the 6-DOF aerial tool system.

### III. CONTROL ALLOCATION UNDER SPHERICAL JOINT CONSTRAINTS

As mentioned above, we want to utilize the thrust of each quadrotor (i.e.,  $\Gamma_i = \lambda_i R_0^T R_i e_3$ ) to generate the desired control action  $U \in \mathbb{R}^6$  for the tool dynamics while respecting the spherical joint limit constraints (1). This problem can be formulated as the following constrained optimization problem:

$$\min_{\Gamma_1, \Gamma_2, \dots, \Gamma_n \in \mathbb{R}^3} \frac{1}{2} \Gamma^T \Gamma \quad (6)$$

subject to

$$B\Gamma = \bar{R}^{-1}U =: \begin{bmatrix} F_d \\ M_d \end{bmatrix} \quad (7)$$

$$p_i^T \Gamma_i \geq |\Gamma_i| \cos \phi_i, i = 1, 2, \dots, n$$

where the first condition of (7) is to generate the desired control action  $[F_d; M_d] \in \mathbb{R}^6$  and the second condition is the spherical joint constraints. This constrained optimization is convex, and also similar to the well-known robot

grasping problem under friction-cone constraint, with many algorithms available to solve it in real-time (e.g., [11]).

Now, let us examine the first condition of (7). There, since  $[F_d; M_d] := \bar{R}^{-1}U \in \mathbb{R}^6$  can be thought of as a given arbitrary control command, the existence of its solution depends on the rank of the matrix  $B \in \mathbb{R}^{6 \times 3n}$ . However, as can be seen from (4),  $B(r)$  is a function of only mechanical design parameters  $r_i$  (i.e., the attaching point of each quadrotor). In other words, this  $r_i$  affects the structure of  $B$ , which in turn decides the existence of solution for (7). This suggests us to choose these mechanical design parameter  $r_i$  s.t.,

$$\text{rank}(B) = 6 \quad (8)$$

If this condition is satisfied, we say the 6-DOF tool dynamics (4) is **fully-actuated**, otherwise **under-actuated**. The next Prop. 1 shows that the number of quadrotors connected to the tool (i.e.,  $n$ ) and their attaching points (i.e.,  $r_i \in \mathbb{R}^3$ ) dictate the full-actuation condition (8) of the 6-DOF tool dynamics.

**Proposition 1:** Consider the system consisting of  $n$  quadrotors connected to a tool by spherical joints with the dynamics (3). Then the 6-DOF tool dynamics (4) is fully-actuated in the sense of (8) if and only if there are at least three quadrotors, whose attaching points  $r_i$  to the tool are not collinear with each other (i.e.,  $(r_2 - r_1) \times (r_3 - r_1) \neq 0$ ). Otherwise, the 6-DOF tool dynamics (4) is under-actuated.

*Proof:* First, we consider the case where there are three quadrotors attached to the tool, whose attaching points to the tool (i.e.,  $r_i$ ) are not collinear as stated above. Then, the control generated by these quadrotors is given by

$$B\Gamma = \underbrace{\begin{bmatrix} I & I & I \\ S(r_1) & S(r_2) & S(r_3) \end{bmatrix}}_{:=B} \underbrace{\begin{bmatrix} \lambda_1 R_0^T R_1 e_3 \\ \lambda_2 R_0^T R_2 e_3 \\ \lambda_3 R_0^T R_3 e_3 \end{bmatrix}}_{:=\Gamma}$$

where we can decompose  $B$  s.t.,

$$B = \underbrace{\begin{bmatrix} I & 0 \\ S(r_1) & I \end{bmatrix}}_{:=L} \underbrace{\begin{bmatrix} I & 0 & 0 \\ 0 & S(r_2 - r_1) & S(r_3 - r_1) \end{bmatrix}}_{:=\Sigma} \underbrace{\begin{bmatrix} I & I & I \\ 0 & I & 0 \\ 0 & 0 & I \end{bmatrix}}_{:=H}$$

We can then see that  $\text{rank}(B) = \text{rank}(\Sigma)$  since  $L$  and  $H$  are full-rank. Thus, if  $(r_2 - r_1) \times (r_3 - r_1) \neq 0$ , we have  $\text{rank}(\Sigma) = 6 = \text{rank}(B)$ . Consider also the case that there are only two quadrotors or more than three quadrotors, yet, their attaching points are all collinear. We then have  $\text{rank}(B) = \text{rank}(\Sigma) = 5$ , i.e., the tool dynamics is under-actuated. This completes the proof. ■

Now, suppose that we have three quadrotors attached to the tool satisfying Prop. 1 as shown in Fig 1. This then ensures that there exists a solution  $\Gamma_i \in \mathbb{R}^3$  to produce the desired tool control input  $U \in \mathbb{R}^6$ . What is unclear though is whether this thrust input vector  $\Gamma_i$  will also respect the motion limit of the spherical joints, i.e., the second condition of (7). This problem is indeed similar to the robot grasping with friction contacts [13], in the sense that we want our tool in the force-closure with the thrust forces  $\Gamma_i$  lying inside the spherical joint limit cone  $(p_i, \phi_i)$ . The following Prop. 2, which is from [13], is due to this similarity between our tool system under spherical joint limit constraints and the grasping under friction-cone constraints.

**Proposition 2:** For the system of three quadrotors satisfying Prop. 1, we can generate any desired control  $U \in \mathbb{R}^6$

in (4) using the thrust inputs  $\Gamma_i \in \mathbb{R}^3$  while respecting the spherical joint limits (1), if and only if the tool is in force-closure with the contact forces  $\Gamma_i$  lying inside the spherical joint limit cone (1).

The Prop. 1 and Prop. 2 can provide a suggestion on how to choose the mechanical design parameters  $r_i$  and  $p_i$  to better generation of control actuation. Even if one of these Prop. 1 or Prop. 2 is not granted, we may still produce some motions, which will be limited, yet, may be still useful. One of the key challenges in the presence of this under-actuation problem is that there may be no solution for the optimization problem (6)-(7). For example, for S2QT system, as shown in Sec. IV-A, the tool is under-actuated, yet, still exhibit useful motions. For this, we also provide a closed-form solution of the optimization problem (6)-(7), which, of course, can accommodate only some limited possible control actions  $[F_d; M_d]$ . In contrast, for the case of S3QT system, all conditions of Prop. 1 and Prop. 2 are satisfied (with enough thrust magnitudes), for which we can utilize the rich literature of optimization to generate any 6-DOF tool behavior as illustrated in the control design example in Sec. IV-B.

#### IV. TOOL OPERATION CONTROL DESIGN EXAMPLES

In this section, we address the control problems of tool-tip pose tracking of the under-actuated S2QT system and the fully-actuated S3QT system.

##### A. Under-actuated S2QT System

As mentioned in Sec. III, the 6-DOF tool with two quadrotors connected via spherical joints is under-actuated. However, as shown below, we can still utilize this S2QT system to generate some limited, yet, useful behaviors, that is, controlling the tool-tip Cartesian position while maintaining a certain desired orientation. For this purpose, we utilize two identical quadrotors, which are symmetrically attached to the tool as shown in Fig. 3 with the following mechanical design parameters:

$$r_1 = -r_2 = -\bar{r}e_1, \quad p_1 = p_2 = e_3 \quad (9)$$

where  $\bar{r} > 0$  is the distance from the quadrotor to the tool's center-of-mass and  $e_1 = [1; 0; 0] \in \mathbb{R}^3$  is the unit vector along the  $N$ -axis.

Here, for simplicity of control derivation/analysis, we also assume that the tool-tip position  $y \in \mathbb{R}^3$  is located on the line connecting the center-of-mass positions of the two quadrotors, with its position specified by  $d = \bar{d}e_1 \in \mathbb{R}^3$  in the tool-frame  $\{T\}$  with the distance  $\bar{d} \geq 0$  from  $x_o$  - see Fig. 3. We also assume that the interaction between the tool-tip and the external environment is a point contact with the interaction torque at the tool-tip being negligible, i.e.,  $\tau_e^y \approx 0$ , and the measurement of the contact force  $f_e^y$  available. Even though these assumptions are not precisely in accordance with the real tool system of Fig. 3 (e.g., offset between the line and the tool-tip  $y$  along the body-fixed  $D$ -direction; non-negligible interaction torque at the tool-tip due to deformation), we also found that the tool system, under the control derived with these assumptions, was functioning adequately in real implementation as shown below. Control derivation/analysis with these assumptions completely removed, i.e., control design with parameter uncertainty and imperfect external force measurement/estimation, turns out to be rather involved

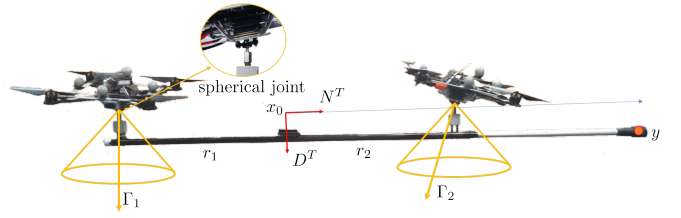


Fig. 3. Prototype of S2QT system with two identical symmetrically-attached quadrotors:  $r_1 = -r_2 = -\bar{r}e_1$  and  $p_1 = p_2 = e_3$ .

due to the presence of under-actuation and will be reported in a future publication.

Our objective is then to control the tool-tip position  $y$  to track a desired trajectory  $y_d \in \mathbb{R}^3$  and the orientation of the tool, represented by  $R_0e_1 \in S^2$ , to converge to a desired orientation  $\gamma_d \in S^2$ . We use the reduced-attitude vectors (i.e.,  $R_0e_1, \gamma_d \in S^2$ ) here instead of rotation matrices (e.g.,  $R_0, R_d \in SO(3)$ ), since the rotation about the pointing direction (i.e.,  $R_0e_1, \gamma_d$ ) is not intended. Note also that, similar to the single quadrotor tool operation [4], we need to simultaneously control the translation (i.e.,  $x_0$ ) and the rotation (i.e.,  $R_0$ ) of the tool. For the case of quadrotor-tool system [4], its under-actuation can induce unstable internal dynamics and even finite-time escape. In contrast to that, for our tool system with two quadrotors, due to the presence of more actuators and the gravity, we do not encounter with a similar issue of internal dynamics instability problem despite of its under-actuation.

To design the control, we first write down the kinematic relation between the tool-tip position  $y$  and the tool center-of-mass  $x_0$  in the fixed frame  $\{O\}$

$$\begin{aligned} y &= x_0 + R_0d \\ \dot{y} &= \dot{x}_0 + R_0S(\omega_0)d \end{aligned} \quad (10)$$

where we can consider  $\dot{x}_0$  and  $\omega_0$  as the control inputs. Let us define the desired value of  $\dot{x}_0$  to be  $\dot{x}_d$  s.t.,

$$\dot{x}_d := -k_y(y - y_d) + \dot{y}_d \quad (11)$$

In general,  $\dot{e}_x := \dot{x}_0 - \dot{x}_d \neq 0$ . With this, we can rewrite (10) s.t.,

$$\dot{e}_y + k_y e_y = \dot{e}_x + R_0S(\omega_0)d \quad (12)$$

where  $e_y = y - y_d$ . We can then see that, if we can achieve  $\dot{e}_x \rightarrow 0$  and  $R_0S(\omega_0)d \rightarrow 0$ , we will have  $e_y \rightarrow 0$  exponentially. Also, if  $\omega_0(t) \rightarrow 0$ , we can further conclude that  $e_R := R_0e_1 - \gamma_d \rightarrow 0$  asymptotically. These are the key ideas of the following Th. 1.

**Theorem 1:** Consider the S2QT system (4) as stated above. Then,  $(e_y, \dot{e}_x) \rightarrow 0$  exponentially and  $(\omega_0, e_R) \rightarrow 0$  asymptotically, if the following condition is satisfied:

$$\begin{bmatrix} I & I \\ S(r_1) & S(r_2) \end{bmatrix} \begin{bmatrix} \Gamma_1 \\ \Gamma_2 \end{bmatrix} = \begin{bmatrix} F_d \\ M_d \end{bmatrix} \quad (13)$$

with

$$\begin{aligned} F_d &:= R_0^T e_y - \sum_{i=0}^2 m_i R_0^T \dot{x}^d + \sum_{i=0}^2 m_i g R_0^T e_3 + k_x R_0^T \dot{e}_x + R_0^T f_e^y \\ M_d &:= -S(d) R_0^T e_y + k_\omega \begin{bmatrix} 0 \\ \omega_{0y} \\ \omega_{0z} \end{bmatrix} - k_R S(e_1) R_0^T \gamma_d + S(d) R_0^T f_e^y \end{aligned}$$

where  $\omega_{0y}, \omega_{0z}$  are the second and third components of  $\omega_0 \in \mathbb{R}^3$ , respectively,  $e_1 = [1, 0, 0]^T \in \mathbb{R}^3$  and  $\gamma_d \in S^2$  is the desired orientation.

*Proof:* Let us define the Lyapunov function:

$$V_1 = \frac{1}{2}e_y^T e_y + \frac{1}{2} \sum_{i=1}^2 m_i \dot{e}_x^T \dot{e}_x + \frac{1}{2} \omega_0^T (J_0 - \sum_{i=1}^2 m_i S^2(r_i)) \omega_0 + k_R (1 - \gamma_d^T R_0 e_1)$$

where  $J_0 - \sum_{i=1}^2 m_i S^2(r_i)$  is positive definite since

$$-S^2(r_1) = -S^2(r_2) = \bar{r} \begin{bmatrix} 0 & 0 & 0 \\ 0 & 1 & 0 \\ 0 & 0 & 1 \end{bmatrix}$$

and  $\gamma_d^T R_0 e_1 \leq 1$ .

Taking the derivative of  $V$  along (4), we then have:

$$\begin{aligned} \dot{V}_1 &= e_y^T (-k_y e_y + \dot{e}_x + R_0 S(\omega_0) d) - k_R \gamma_d^T R S(\omega_0) e_1 \\ &\quad + \dot{e}_x^T (\sum_{i=0}^2 m_i g e_3 + f_e^y - \sum_{i=1}^2 \lambda_i R_i e_3 - \sum_{i=0}^2 m_i \ddot{e}_x^d) \\ &\quad + \omega_0^T (-\sum_{i=1}^2 \lambda_i S(r_i) R_0^T R_i e_3 + S(d) R_0^T f_e^y) \end{aligned}$$

Further, if we insert the condition (13) into the above relation, we have:

$$\dot{V}_1 = -k_y e_y^T e_y - k_x \dot{e}_x^T \dot{e}_x - k_\omega [\omega_{0y}^2 + \omega_{0z}^2] \leq 0$$

This implies  $(e_y, \dot{e}_x) \rightarrow 0$  exponentially and  $\omega_0$  are bounded. Similar to [14], we can establish  $(\omega_0, e_R) \rightarrow 0$  asymptotically. This completes the proof. ■

Now, given the target control action  $\bar{R}^{-1}U := [F_d; M_d]$  as computed in Th. 1, the next task is to allocate this  $U$  into each quadrotor thrust control  $\Gamma_i = \lambda_i R_0^T R_i e_3 \in \mathbb{R}^3$  while respecting the spherical joint constraints (1), that is, solving the constrained optimization problem (6)-(7). Of course, due to the under-actuation of this two-quadrotor tool system, not all the 6-DOF motion is attainable. In fact, due to the under-actuation, this S2QT system can only control 5-DOF motion, with the 1-DOF rotation along the body-fixed  $N$ -direction not directly controllable. If we do not consider this kind of limitation, the constrained optimization (6)-(7) can suffer from the non-existence of solutions. To avoid this, we intentionally set the first row of  $M_d$  in Th. 1 to be zero, i.e.,  $e_1^T M_d = 0$ , with  $d = \bar{d} e_1$ ,  $e_1^T S(e_1) R_0^T \gamma_d = 0$ ,  $e_1^T S(d) R_0^T f_e^y = 0$  and  $e_1^T S(d) R_0^T e_y = 0$ . Note that, with the desired pointing direction (i.e.,  $\gamma_d \in S^2$ ), the information of rotation about this pointing direction is reduced. It is also worthwhile to mention that this un-actuated rotation about the  $N$ -direction in tool frame (i.e.,  $R_0 e_1$ ) is still stabilized due to gravity, similar to the case of stable pendulum [14].

Now, for given  $F_d, M_d$ , we can also explicitly solve the second and third components of  $\Gamma_1, \Gamma_2$  from (13) s.t.,

$$\begin{bmatrix} \Gamma_{1y} \\ \Gamma_{1z} \\ \Gamma_{2y} \\ \Gamma_{2z} \end{bmatrix} = \frac{1}{2} \begin{bmatrix} F_{dy} - M_{dz}/\bar{r} \\ F_{dz} + M_{dy}/\bar{r} \\ F_{dy} + M_{dz}/\bar{r} \\ F_{dz} - M_{dy}/\bar{r} \end{bmatrix}$$

where  $\Gamma_i = [\Gamma_{ix}; \Gamma_{iy}; \Gamma_{iz}] \in \mathbb{R}^3$  and  $F_d = [F_{dx}; F_{dy}; F_{dz}] \in \mathbb{R}^3$ . This means that for given  $F_d, M_d$ , there exists unique solution for  $\Gamma_{1y}, \Gamma_{1z}, \Gamma_{2y}, \Gamma_{2z}$ , which can be explained as following. Given the force along the  $E$ -axis  $F_{dy}$  and the torque about the  $D$ -axis  $M_{dz}$ , we need a pair of

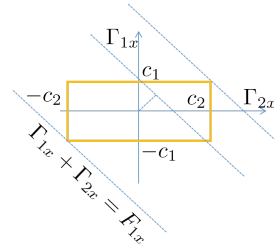


Fig. 4. Geometry of the simplified optimization problem (14)-(15).

forces along the  $E$ -axis  $\Gamma_{1y}, \Gamma_{2y}$  to balance them. Similarly, given  $F_{dz}, M_{dy}$ , we need a pair of forces along the  $D$ -axis  $\Gamma_{1z}, \Gamma_{2z}$ .

Then, with  $\Gamma_{1y}, \Gamma_{1z}, \Gamma_{2y}, \Gamma_{2z}$  as determined above, we can further simplify the optimization problem (6)-(7) s.t.,

$$\min_{\Gamma_{1x}, \Gamma_{2x} \in \mathbb{R}} \frac{1}{2} (\Gamma_{1x}^2 + \Gamma_{2x}^2) \quad (14)$$

subject to

$$\begin{aligned} \Gamma_{1x} + \Gamma_{2x} &= F_{dx} \\ \Gamma_{ix}^2 &\leq \underbrace{\frac{1 - \cos^2 \phi_i}{\cos^2 \phi_i} \Gamma_{iz}^2 - \Gamma_{iy}^2}_{=: c_i^2}, \quad i = 1, 2 \end{aligned} \quad (15)$$

with  $c_1, c_2$  are assumed to be positive real numbers here.

Geometric structure of this optimization problem (14)-(15) is shown in Fig. 4, from which we can then see that, if  $|F_{dx}| \leq c_1 + c_2$ , the solution has the following closed-form expression:

$$\Gamma_{1x} = \frac{1}{2} F_{dx} + \zeta, \quad \Gamma_{2x} = \frac{1}{2} F_{dx} - \zeta$$

where

$$\zeta := \begin{cases} 0 & \text{if } \frac{1}{2}|F_{dx}| \leq \min(c_1, c_2) \\ \frac{1}{2}F_{dx} - c_2 & \text{if } \frac{1}{2}|F_{dx}| > \min(c_1, c_2), \quad c_1 \geq c_2 \\ -\frac{1}{2}F_{dx} + c_1 & \text{if } \frac{1}{2}|F_{dx}| > \min(c_1, c_2), \quad c_1 < c_2 \end{cases} \quad (16)$$

Of course, there may be a certain behavior which may be too aggressive to be realized by the two quadrotors with limited spherical joint motions. More precisely, from Fig. 4, we can conclude that, if one of the following conditions is granted, no solution exists for  $\Gamma_1, \Gamma_2$ , that produces the desired control action while respecting the spherical joint constraints:

$$|F_{dx}| > c_1 + c_2, \quad \frac{1 - \cos^2 \phi_i}{\cos^2 \phi_i} \Gamma_{iz}^2 - \Gamma_{iy}^2 < 0, \quad i = 1, 2$$

This means that, with the under-actuated S2QT system, we can generate only some limited desired tool control  $F_d, M_d$ . For controlling more complex motion, we need to have a fully-actuated 6-DOF tool system satisfying both Prop. 1 and 2, for instance, the S3QT system presented in Sec. IV-B.

*Remark 1:* The obtained thrust inputs,  $\Gamma_1, \Gamma_2$  via the constrained optimization (6)-(7), should then be produced by each quadrotor via their individual control inputs  $(\lambda_i, \omega_i)$  or  $(\lambda_i, \tau_i)$ . Here, the magnitude of  $\Gamma_i$  can be directly attained by  $\lambda_i$ , yet, the direction of  $\Gamma_i$  should be achieved by aligning its orientation  $R_i$  through  $\omega_i$  or  $\tau_i$ . There are many available control techniques for this. For the implementation below, we adopt the backstepping control of [15].

To validate the theory, we here perform preliminary experiments for this S2QT system. The quadrotors used are

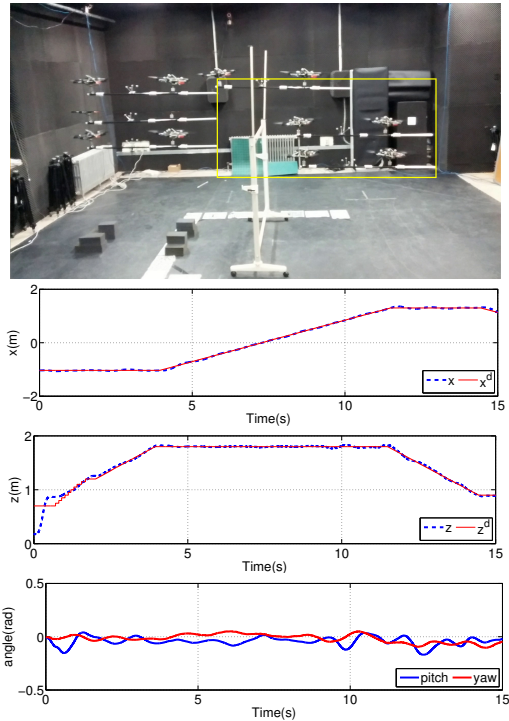


Fig. 5. S2QT system: tool-tip tracking a vertical rectangular-like shape while maintaining a certain attitude (e.g., pitch and yaw all zero).

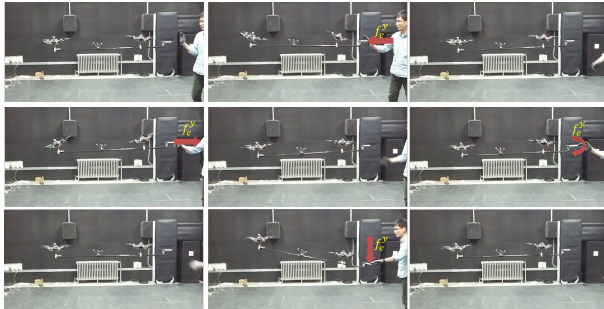


Fig. 6. Impedance control of S2QT system with external forces along N/D/E-directions.

AscTec Hummingbirds, where the weight is about 0.6 kg, the recommended payload is 0.2 kg and the maximum thrust is 20 N. The mechanical design of the system is shown in Fig. 3, where the spherical joints are at the quadrotor center-of-masses to satisfy the assumption in Sec. II. The spherical joints used here has the range of angle motion  $\phi_i = 32^\circ$ . The weight of the tool and joints are 0.34 kg. With this system in Fig. 3, we could obtain the maximum horizontal force of approximately 14 N while maintaining hovering, which is fairly high as compared to other aerial manipulation systems (e.g., 6 N contact force of [8]). In these preliminary experiments, we use VICON motion capture system to measure the attitudes of the tool and the quadrotors, and the translation of the tool. How to obtain these quantities without motion capture system, e.g., using IMU and optical flow [16], is a topic of future development.

The scenario for experiment aims at showing that the attitude of the tool can be maintain while tracking desired motion of the tool-tip. As stated in Sec. IV-A, although, for the prototype of Fig. 3, the tool-tip is not on the line connecting the two center-of-masses of quadrotors, the system

performs adequately as can be seen below. The scenario and tracking errors for this S2QT system are presented in Fig. 5. We can see that, without the presence of external force, the tool-tip tracks the desired trajectory fairly well, with the error less than 5 cm while maintaining the desired attitude. During the flight, we observed that the tool maintains the desired pose due to the gravity stabilization [14]. In case the tool-tip is on the line connecting two center-of-masses of the quadrotors, the system can stably resist external forces acting on the tool ( $\tau_e^y \approx 0$ ), as shown in Fig 6. Experiment videos with different scenarios can be found at the following URL: <http://inrol.snu.ac.kr/iros2015>.

### B. Fully-actuated S3QT System

Here, we consider the problem of the tool-tip position/orientation control of the fully-actuated 6-DOF tool system with three quadrotors. Let us define the desired tool-tip pose as  $(y_d, R_d) \in SE(3)$  represented in the inertial frame  $\{O\}$ . Note that,  $R_d \in SO(3)$  here can be chosen arbitrary in contrast to the case of two quadrotors of Sec. IV-A, for which we restrict ourselves to a desired pointing direction  $\gamma_d \in S^2$  with the rotation around  $\gamma_d$  being neglected.

Our control objective is  $(y, R_0) \rightarrow (y_d, R_d)$ . As stated in Sec. III, for the three quadrotors, as long as each quadrotor can produce enough thrust, we can always find the desired thrust input  $\Gamma_i$  for each quadrotor, that can generate the desired wrench for the tool  $[F_d; M_d]$  while also respecting the spherical joint limits, as the system can always satisfy Prop. 1 and Prop. 2 in this case.

Similar to Sec. IV-A, we start with the kinematic relation:

$$\dot{y} = \dot{x}_0 + R_0 S(\omega_0) \quad (17)$$

with  $d = [d_1; d_2; d_3] \in \mathbb{R}^3$  is the tool-tip position expressed in the tool-frame  $\{T\}$ . Here, differently from the case of two-quadrotor tool system in Sec. IV-A, we assume an arbitrary vector  $d \in \mathbb{R}^3$  for the tool-tip position, since, in this case, with the full-actuation with three quadrotors, such a general  $d$  does not make the control derivation/analysis any more complicated in comparation to the case of  $d = de_1$  in Sec. IV-A. Then, similar to the procedure of Sec. IV-A, using  $\dot{x}_0, \omega_0$  as the control input, we can again enforce  $(y, R_0) \rightarrow (y_d, R_d)$  as summarized in the following Th. 2.

**Theorem 2:** Consider the S3QT system (4) as stated above. Then, we have  $(y, R_0) \rightarrow (y_d, R_d)$  asymptotically, if the following conditions are satisfied:

$$\begin{bmatrix} I & I & I \\ S(r_1) & S(r_2) & S(r_3) \end{bmatrix} \begin{bmatrix} \Gamma_1 \\ \Gamma_2 \\ \Gamma_3 \end{bmatrix} = \begin{bmatrix} F_d \\ M_d \\ \Gamma_3 \end{bmatrix} \quad (18)$$

where

$$F_d := R_0^T e_y - \sum_{i=0}^3 m_i R_0^T \ddot{x}^d + \sum_{i=0}^3 m_i g R_0^T e_3 + k_x R_0^T \dot{e}_x$$

$$+ \sum_{i=1}^3 m_i S(\omega_0) S(r_i) \omega_0 + R_0^T f_e$$

$$M_d := -S(d) R_0^T e_y + k_\omega \omega_0 + k_R [R_0^T R_d - R_d^T R_0]^\vee$$

$$+ \sum_{i=1}^3 m_i g S(r_i) R_0^T e_3 + \tau_e$$

and  $[\star]^\vee$  is denoted  $[\star]^\vee : \mathfrak{so}(3) \rightarrow \mathbb{R}^3$ .

*Proof:* Let us define the Lyapunov function:

$$V_2 = \frac{1}{2} e_y^T e_y + \frac{1}{2} [\dot{e}_x^T \quad \omega_0^T] M [\dot{e}_x \quad \omega_0] + k_R (3 - \text{trace}(R_0^T R_d))$$

We then have:

$$\begin{aligned} \dot{V}_2 &= -k_y e_y^T e_y + \omega_0^T \tau_e + \dot{e}_x^T (e_y - \sum_{i=0}^3 m_i \ddot{x}^d + f_e) \\ &\quad + \omega_0^T [-\sum_{i=1}^3 \lambda_i S(r_i) R_0^T R_i e_3 + S(d) R_0^T e_y + \sum_{i=1}^3 m_i g S(r_i) R_0^T e_3] \\ &\quad + \dot{e}_x^T [\sum_{i=0}^3 m_i g e_3 + \sum_{i=1}^3 m_i R_0 S(\omega_0) S(r_i) \omega_0 - \sum_{i=1}^3 \lambda_i R_i e_3] \\ &\quad + k_R \omega_0^T [R_0^T R_d - R_d^T R_0]^\vee \end{aligned}$$

Using condition (18), we further have

$$\dot{V}_2 = -k_y e_y^T e_y - k_x \dot{e}_x^T \dot{e}_x - k_\omega \omega_0^T \omega_0 \leq 0$$

and  $\dot{V}_2 = 0$  when  $(e_y, \dot{e}_x, \omega_0) = 0$ . Then, similar to Sec. IV-A, we can show that  $(e_y, \dot{e}_x) \rightarrow 0$  exponentially. Also, using the result of [17], we have  $(\omega_0, R_0) \rightarrow (0, R_d)$  asymptotically. This completes the proof. ■

Once we have the target control input  $[F_d; M_d]$  as stated in Th. 2, we can then obtain  $\Gamma_i$  by solving the constrained optimization problem (6)-(7), which, as mentioned above, always has a solution for this case of three-quadrrotor tool system, as long as each quadrrotor can produce enough thrust magnitude and the mechanical design satisfies Prop. 1 and Prop. 2. For this constrained optimization problem (6)-(7), since it is convex with the structure similar to the well-known robot grasping under friction-cone constraint, we can utilize many available fast/efficient algorithms (e.g., [11]).

Simulation results of this three-quadrrotor tool system with spherical joints are presented in Fig. 7, which clearly support our theoretical claims. Given that the similar setup has been successfully implemented for the S2QT system (Sec. IV-A), we expect it would also be possible to implement this S3QT system, which will be reported in a future publication.

## V. CONCLUSIONS

In this paper, we introduce a new system consisting of multiple quadrotors connected to a tool by spherical joints to perform tool operation tasks. By analyzing the dynamics structure of the system while respecting the spherical joint constraints, we reveal a strong relation between the mechanical design of the system and the (possible) control design of the system. We also address two control design examples on the tool-tip pose tracking control, which is essential to any tool operation tasks. Some future research directions include: 1) control design and implementation of more diverse aerial tool operation scenarios, including S3QT system; 2) improvement on robustness and effectiveness of the SmQT system for outdoor applications.

## REFERENCES

- [1] R. Mahony, V. Kumar, and P. Corke. Multirotor aerial vehicles: Modeling, estimation, and control of quadrotor. *IEEE Robotics & Automation Magazine*, 19(3):20–32, 2012.
- [2] S. Bellens, J. De Schutter, and H. Bruyninckx. A hybrid pose / wrench control framework for quadrotor helicopters. In *Proc. IEEE Int'l Conference on Robotics & Automation*, pages 2269–2274, 2012.
- [3] D. J. Lee and C. Ha. Mechanics and control of quadrotor for tool operation. In *Proc. ASME Dynamic Systems and Control Conference*, pages 177–184, 2012.
- [4] H.-N. Nguyen and D. J. Lee. Hybrid force/motion control and internal dynamics of quadrotors for tool operation. In *Proc. IEEE/RSJ Int'l Conference on Intelligent Robots & Systems*, pages 3458–3464, 2013.
- [5] H.-N. Nguyen, C. Ha, and D. J. Lee. Mechanics, control and internal dynamics of quadrotor tool operation. *Automatica*. Conditionally Accepted.
- [6] N. Michael, J. Fink, and V. Kumar. Cooperative manipulation and transportation with aerial robots. *Autonomous Robots*, 30(1):73–86, 2011.
- [7] J. Fink, N. Michael, S. Kim, and V. Kumar. Planning and control for cooperative manipulation and transportation with aerial robots. *International Journal of Robotics Research*, 30(3):324–334, 2011.
- [8] R. Naldi, A. Ricco, A. Serrani, and L. Marconi. A modular aerial vehicle with redundant actuation. In *Proc. IEEE/RSJ Int'l Conference on Intelligent Robots & Systems*, pages 1393–1398, 2013.
- [9] R. Naldi, F. Forte, A. Serrani, and L. Marconi. Modeling and control of a class of modular aerial robots combining under actuated and fully actuated behavior. *IEEE Transactions on Control Systems Technology*, PP(99):1–1, 2015.
- [10] H. Yang and D. J. Lee. Dynamics and control of quadrotor with robotic manipulator. In *Proc. IEEE Int'l Conference on Robotics & Automation*, pages 5544–5549, 2014.
- [11] S. P. Boyd and B. Wegbreit. Fast computation of optimal contact forces. *IEEE Transactions on Robotics*, 23(6):1117–1132, 2007.
- [12] D. Mellinger, M. Shomin, N. Michael, and V. Kumar. *Cooperative Grasping and Transport Using Multiple Quadrotors*, volume 83 of *Springer Tracts in Advanced Robotics*, chapter 39, pages 545–558. Springer Berlin Heidelberg, 2013.
- [13] J.-W. Li, H. Liu, and H.-G. Cai. On computing three-finger force-closure grasps of 2-d and 3-d objects. *IEEE Transactions on Robotics and Automation*, 19(1):155–161, 2003.
- [14] N. A. Chaturvedi and N. H. McClamroch. Stabilization of under-actuated 3d pendulum using partial angular velocity feedback. In *Proc. IEEE Conference on Decision and Control & European Control Conference*, pages 6818–6823, 2005.
- [15] C. Ha, Z. Zuo, F. B. Choi, and D. J. Lee. Passivity-based adaptive backstepping control of quadrotor-type uavs. *Robotics and Autonomous Systems*, 62(9):1305–1315, 2014.
- [16] V. Grabe, H. H. Bulthoff, and P. R. Giordano. On-board velocity estimation and closed-loop control of a quadrotor uav based on optical flow. In *Proc. IEEE Int'l Conference on Robotics & Automation*, pages 491–497, 2012.
- [17] A. Sarlette, R. Sepulchre, and N. E. Leonard. Autonomous rigid body attitude synchronization. *Automatica*, 45(2):572–577, 2009.

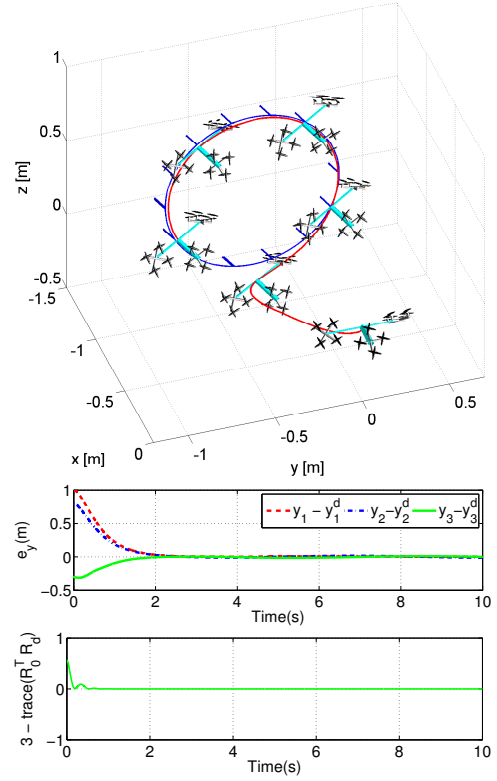


Fig. 7. Simulation result of tool-tip pose control of S3QT system.